Medicinal Chemistry Research
https://doi.org/10.1007/s00044-018-2154-4

MEDICINAL CHEMISTRY RESEARCH

ORIGINAL RESEARCH

Synthesis, crystal structure, and antinociceptive effects of some new riluzole derivatives

Xiang-Long Wu[1] · Liu Liu[1] · You-Jia Li[1] · Jie Luo[1] · Dong-Wei Gai[1] · Ting-Li Lu[1] · Qi-Bing Mei[1]

Received: 28 September 2017 / Accepted: 10 February 2018

Abstract

Nine N-alkylated derivatives of riluzole were synthesized in order to obtain new compounds with potential antinociceptive activity. Riluzole was firstly transformed into (6-trifluoromethoxy-benzothiazol-2-yl)-hydrazine, then it was chlorinated by $SOCl_2$ to obtain 2-chloro-6-trifluoromethoxy-benzothiazole. This intermediate product was treated with nine alkylamines to give N-alkylated derivatives of riluzole respectively. The structures of compounds were confirmed by means of elemental analysis, IR, ^{1}H NMR, and ^{13}C NMR. The synthetic route was optimized and four novel crystals were obtained by recrystallization. This study investigated the antinociceptive activity of some N-alkylated derivatives of riluzole by hot plate test in mice. The relationship between antinociceptive activity and the doses of **4b**, **4c**, **4h**, **4g**, and riluzole had been studied. Compared with the control group (0 mg/kg), the effects of compounds **4b** and **4h** showed a significant increase (13.78 ± 2.89 s, 12.89 ± 2.94 s, respectively). Compound **4c** showed extreme significant increase (18.07 ± 3.08 s) in the time mice spent on the hot plate. The compounds **4b**, **4c**, and **4h** had increased the latency time compared to the blank solvent group. They have potential application in developing new drug candidates with antinociceptive activity.

Keywords Riluzole · Benzothiazole derivatives · Antinociceptive · Synthesis · Crystal structure

Introduction

Riluzole [2-amino-6-(trifluoromethoxy) benzothiazole], is a derivative of benzothiazole, a bicyclic ring compound, which comprises a benzene ring, fused to a five-membered ring containing one nitrogen and one sulfur atom (Cheah et al. 2010). Riluzole, a novel anti-glutamate agent with neuroprotective properties in animal models of neurodegenerative disease, has been approved by the U.S. Food and Drug Administration for amyotrophic lateral sclerosis (Cheung et al. 2006). It is effective in animal models of Parkinson's disease, Huntington's disease and cerebral and retinal ischemia (Jehle et al. 2000).

2-(N-alkylamino) benzothiazoles exhibit a wide range of pharmacological and physiological activities, and they are very important structural units in many biologically active compounds. Benzothiazole derivatives were first identified as potential muscle relaxants in clinical medicine during the 1950s (Domino et al. 1952). Research into benzothiazole derivatives subsequently subsided, although interest was reignited with identification of the anti-convulsant properties of riluzole during the 1980s (Mizoule et al. 1985). Benzothiazole derivatives have demonstrated anti-tumor, antimicrobial, anti-helmintic, anti-leishmanial, anti-inflammatory, and psychotropic properties (Rana et al. 2007).

Riluzole can delay the onset of thermal and tactile hypersensitivity and partially reverse established pain behavior. It also can reduce microglial staining in the spinal cord (Chew et al. 2014). Riluzole has undergone clinical trials for spinal cord injury, and the promising results obtained here suggest that its use may provide a new treatment option for avulsion injuries, a very specific type of spinal cord injury (Wilson and Fehlings 2013). Early administration of riluzole is sufficient to relieve nerve root-mediated pain by preventing development of neuronal

Electronic supplementary material The online version of this article (https://doi.org/10.1007/s00044-018-2154-4) contains supplementary material, which is available to authorized users.

✉ Ting-Li Lu
lutinglixinxin@nwpu.edu.cn

✉ Qi-Bing Mei
gahpyudx@163.com

[1] Key Laboratory for Space Bioscience and Biotechnology, School of Life Sciences, Northwestern Polytechnical University, 710072 Xi'an, China

Published online: 02 March 2018

dysfunction in the spinal cord and the nerve root (Nicholson et al. 2014). Riluzole improved functional recovery and preserved tissue in a rat model of mild gradual cervical spinal cord compression. It can inhibit the induction and maintenance of neuropathic pain. Riluzole represents a novel therapeutic approach to attenuate neuropathic pain and protect against neurological loss in cervical spondylotic myelopathy (Moon et al. 2014).

Riluzole and other benzothiazoles protect against transcriptional impact and adverse molecular networks following neuronal stress (Liu et al. 2011). Suitability of riluzole for symptom relief, as well as potential for prevention of neurodegenerative consequences associating visceral hypersensitivity do provide a new class of specific therapeutic agent for treating irritable bowel syndrome (Mishra et al. 2014). 2-Amino-6-trifluoromethylthio-benzothiazole (SKA-19), a thioanalog of riluzole, as a potent, novel anticonvulsant, had been reported. It exerts broad spectrum anticonvulsant and analgesic effects (Coleman et al. 2015). Given the function of riluzole and benzothiazole derivatives, we designed and synthesized nine N-alkylated derivatives of riluzole.

The direct N-alkylation of 2-amino-benzothiazole is one of the easiest methods for the preparation of 2-(N-alkylamino) benzothiazole. However, such reactions with alkyl halides afford 3-alkyl-2-imino-benzothiazolines other than 2-(N-alkylamino) benzothiazole because the endocyclic nitrogen is more basic than the exocyclic one (Jimonet et al. 1999). Several transition metal-catalyzed methods have been developed for the synthesis of 2-(N-alkylamino) benzothiazoles, including oxidative C–H funcationalization of benzothioureas (Joyce and Batey 2009), cyclization of ortho- halobenzothioureas (Saha et al. 2009), and oxidative decarbonylative coupling of benzothiazoles with formamides. However, these methods usually suffer from the multistep synthesis of the starting materials, use of expensive metal catalysts and low functional group tolerance.

In this paper, we will report a revised approach to N-alkylated derivatives of riluzole according to the reference (Mignani et al. 1992). Nine N-alkylated derivatives of riluzole were obtained. To our knowledge, **4b**, **4d**, **4e**, **4f**, **4g**, **4h**, and **4i** were new compounds. To investigate the antinociceptive activity of N-alkylated derivatives of riluzole, the hot plate test was performed, which was a selective test that uses heat as a nociceptive stimulus to identify analgesic substances with a central effect.

Materials and methods

Experimental general information

Melting points were measured on a X-4 micro melting point apparatus. IR spectra in cm^{-1} were recorded on a Brucker Equiox-55 FTIR spectrometer. ^{1}H and ^{13}C spectra were recorded on a BRUKER AVANCE instrument. Elemental analyses for C, H, and N were obtained using a Vario EL-III analyzer. The X-ray diffraction data were collected on a Bruker SMART AREX II CCD diffractometer equipped with a graphite monochromated Mo Kα radiation ($\lambda =$ 0.071073 nm) source by using the ω-2θ scan technique at room temperature. The structure was solved by direct methods with SHELXS-97, and refined used SHELXL-97. Crystallographic data for the structures reported here have been deposited with CCDC (Deposition No. CCDC-1039246 (**3**), CCDC-1453892 (**4e**), CCDC-1045917 (**4f**), and CCDC-1446747(**4i**)). These data can be obtained free of charge via http://www.ccdc.cam.ac.uk/conts/retrieving.html or from CCDC, 12 Union Road, Cambridge CB2 1EZ, UK, E-mail: deposit@ccdc.cam.ac.uk.

Synthesis of (6-trifluoromethoxy-benzothiazol-2-yl)-hydrazine (2)

6-Trifluoromethoxy-2-amino-benzothiazole (23.42 g, 0.10 mol), hydrazinium sulfate ($NH_2NH_2 \bullet H_2SO_4$, 19.52 g, 0.15 mol) and hydrazine hydrate (80% aqueous solution, 80 mL) were added to ethylene glycol (350 mL). The mixture was heated and stirred under nitrogen at 130 °C for 4 h. TLC (CH_2Cl_2/MeOH = 20:1) was used to confirm the completion of the reaction. After cooling to room temperature, the mixture was poured into the ice-water. A lot of gray solid was precipitated. The precipitate was filtered and washed three times with water. The solid was dried in vacuum to constant weight. Compound **2** (18.7 g, Yield 75%) was obtained. Gray schistose; mp 205–206 °C; IR (KBr) υ_{max} 3362, 3205, 3124, 2963, 2880, 2361, 1660, 1564, 1464, 1261, 1123 cm^{-1}; ^{1}H NMR (DMSO-d_6, 500 MHz): $\delta = 9.22$ (1H, s, –NH–), 7.79 (1H, s, Ar–H), 7.35 (1H, d, $J = 8.7$ Hz, Ar–H), 7.17 (1H, d, $J = 8.7$ Hz, Ar–H), 5.12 (2H, s, $–NH_2$); ESI-MS *m/z* 248.39[M–H]$^-$; $C_8H_6F_3N_3OS$ (calcd. 249.21) Anal. Calcd. for $C_8H_6F_3N_3OS$: C, 38.56; H, 2.43; N, 16.86. Found: C, 38.44; H, 2.34; N, 16.75.

Synthesis of 2-chloro-6-trifluoromethoxy benzothiazole (3)

Compound **2** (12.45 g, 0.05 mol) was slowly added in portions to a solution of $SOCl_2$ (120 mL) which was preheated at 65 °C. The solution was stirred for 5 h at 60 °C. Thionyl chloride was evaporated, then the residue was dissolved in CH_2Cl_2 and solvent was evaporated again. This process was repeated at least three times in order to remove all $SOCl_2$. The residue was dissolved in CH_2Cl_2 and washed three times with water, dried over anhydrous Na_2SO_4. The solvent was removed under reduced pressure. The crude product was purified by column chromatography on silica

gel eluted with petroleum ether (60–90 °C) to give compound **3** (10.71 g, Yield 85%) as a white solid. mp 38–39 °C; IR (KBr) υ_{max} 3099, 3078, 2361, 1480, 1452, 1262, 1164, 1016, 865 cm^{-1}; ^1H NMR ($CDCl_3$, 500 MHz): $\delta = 7.96$ (1H, d, $J = 8.9$ Hz, Ar–H), 7.66 (1H, s, Ar–H), 7.37 (1H, d, $J = 8.9$ Hz, Ar–H); ESI-MS: *m/z* 251.91 $[M–H]^-$; $C_8H_3ClF_3NOS$ (calcd.252.96); Anal. Calcd for $C_8H_3ClF_3NOS$: C, 37.88; H, 1.19; N, 5.52. Found: C, 37.95; H, 1.13; N, 5.59.

General procedure for the preparation of N-alkylated derivatives of riluzole (4a–4i)

2-Chloro-6-trifluoromethoxy-benzothiazole (1.27 g, 5 mmol) was dissolved in 10 mL ethylamine aqueous solution. The resultant mixture was stirred at room temperature overnight. The solvent was removed under reduced pressure. The residue was dissolved in CH_2Cl_2 and washed three times with water, dried over anhydrous Na_2SO_4, filtered and the solvent completely removed. The crude material was purified by column chromatography over silica used dichloromethane as eluent to give compound **4a** as a white amorphous powder (1.11 g, 84.7%). Compounds **4b–4i** were also prepared by the same procedure from compound **3** with *n*-butylamine, diaethylamin, cyclohexylamine, pyrrolidine, piperidine, morpholine, and 4-methylpiperidine, respectively. Spectroscopic data of N-alkylated derivatives of riluzole were given as follow.

2-(N-ethylamine)-6-trifluoromethoxy-benzothiazole (4a)

White solid; mp 133–134 °C; IR (KBr) υ_{max} 3210, 2987, 2922, 2361, 1622, 1584, 1461, 1250, 1214, 1152, 807 cm^{-1}; ^1H NMR ($CDCl_3$, 500 MHz): $\delta = 7.48$ (1H, d, $J = 8.8$ Hz, Ar–H), 7.46 (1H, s, Ar–H), 7.16 (1H, d, $J = 8.8$ Hz, Ar–H), 5.69 (1H, s, –NH–), 3.47 (2H, q, $J = 7.2$ Hz, $–CH_2–$), 1.34 (3H, t, $J = 7.2$ Hz, $–CH_3$); ^{13}C NMR($CDCl_3$, 125 MHz): $\delta = 167.95$ (C, S–C–N), 150.94 (C, Ar–O), 143.57 (C, Ar–N), 130.86 (C, Ar–S), 121.65(C, q, $J = 237.5$ Hz, $–CF_3$), 119.68 (C, Ar-4), 118.92 (C, Ar-5), 114.07 (C, Ar-7), 40.43 (C, N–C–C), 14.83(C, $–CH_3$); Anal. Calcd for $C_{10}H_9F_3N_2OS$: C, 45.80; H, 3.46; N, 10.68. Found: C, 45.93; H, 3.40; N, 10.76.

2-(N-propylamine)-6-trifluoromethoxy-benzothiazole (4b)

White solid; mp 88–89 °C; IR (KBr) υ_{max} 3150, 2978, 2861, 2361, 1614, 1556, 1463, 1281, 1214, 1162, 808 cm^{-1}; ^1H NMR ($CDCl_3$, 500 MHz): $\delta = 7.47$ (1H, d, $J = 8.8$ Hz, Ar–H), 7.45 (1H, s, Ar–H), 7.16 (1H, d, $J = 8.8$ Hz, Ar–H), 5.75 (1H, s, –NH–), 3.39 (2H, t, $J = 7.1$ Hz, NH–$\underline{CH_2}$), 1.75–1.69 (2H, m, $–CH_2\underline{CH_2}CH_3$), 1.02 (3H, t, $J = 7.4$ Hz, $–CH_3$); ^{13}C NMR ($CDCl_3$, 125 MHz): $\delta = 168.23$ (C, S–C–N), 150.98 (C, Ar–O), 143.54 (C, Ar–N), 130.84 (C, Ar–S), 121.65(C, q, $J = 237.5$ Hz, $–CF_3$), 119.68 (C, Ar-4), 118.87 (C, Ar-5), 114.06 (C, Ar-7), 47.44 (C, NH–C–C), 22.79 (C, –C–C),11.34(C, $–CH_3$); Anal. Calcd for $C_{11}H_{11}F_3N_2OS$: C, 47.82; H, 4.01; N, 10.14. Found: C, 47.69; H, 4.20; N, 10.03.

2-(N-n-butylamine)-6-trifluoromethoxy-benzothiazole (4c)

White solid; mp 76–78 °C; IR (KBr) υ_{max} 3211, 2923, 2859, 2361, 1626, 1566, 1462, 1264, 1166, 815 cm^{-1}; ^1H NMR ($CDCl_3$, 500 MHz): $\delta = 7.47$ (1H, d, $J = 8.8$ Hz, Ar–H), 7.45 (1 H, s, Ar–H), 7.15 (1H, d, $J = 8.7$ Hz, Ar–H), 5.74 (1H, s, –NH–), 3.41 (2H, t, $J = 7.1$ Hz, $NH\underline{CH_2}$), 1.71–1.65 (2H, m, $NHCH_2\underline{CH_2}$), 1.48–1.41 (2H, m, $–\underline{CH_2}CH_3$), 0.96 (3H, t, $J = 7.4$ Hz, CH_3); Anal. Calcd for $C_{12}H_{13}F_3N_2OS$: C, 49.65; H, 4.51; N, 9.65. Found: C, 49.54; H, 4.46; N, 9.69.

2-(N-diaethylamine)-6-trifluoromethoxy-benzothiazole (4d)

White solid; mp 38–39 °C; IR (KBr) υ_{max} 3090, 2981, 2938, 2857, 2361, 1607, 1550, 1460, 1359, 1294, 1215, 1151 cm^{-1}; ^1H NMR (Acetone-d_6, 500 MHz): $\delta = 7.72$ (1H, s, Ar–H), 7.46 (1H, d, $J = 8.8$ Hz, Ar–H), 7.21 (1H, d, $J = 8.8$ Hz, Ar–H), 3.62 (4H, q, $J = 7.1$ Hz, $2 \times –CH_2–$), 1.27 (6H, t, $J = 7.1$ Hz, $2 \times –CH_3$); ^{13}C NMR ($CDCl_3$, 100 MHz): $\delta = 167.81$ (C, S–C–N), 152.15 (C, Ar–O), 142.94 (C, Ar–N), 131.27 (C, Ar–S), 121.94(C, q, $J = 246$ Hz, $–CF_3$), 119.50 (C, Ar-4), 118.64 (C, Ar-5), 113.76 (C, Ar-7), 45.52 (C, N–C–C), 12.80 (C, $–CH_3$); Anal. Calcd for $C_{12}H_{13}F_3N_2OS$: C, 49.65; H, 4.51; N, 9.65. Found: C, 49.54; H, 4.62; N, 9.77.

2-(N-cyclohexylamine)-6-trifluoromethoxy-benzothiazole (4e)

White solid; mp 96–97 °C; IR (KBr) υ_{max} 3427, 3231, 2933, 2858, 1616, 1548, 1456, 1249, 1220, 1162 cm^{-1}; ^1H NMR ($CDCl_3$, 500 MHz): $\delta = 7.46$ (1H, d, $J = 8.8$ Hz, Ar–H), 7.44 (1H, s, Ar–H), 7.15 (1H, d, $J = 8.7$ Hz, Ar–H), 5.53 (s, 1H, –NH–), 3.56 (1H, t, $J = 9.6$ Hz, –CH–), 2.14–2.10(2H, m, $–CH_2–$), 1.80–1.76 (2H, m, $–CH_2–$), 1.52–1.14 (6H, m, $3 \times –CH_2–$); ^{13}C NMR($CDCl_3$, 100 MHz): $\delta = 167.12$ (C, S–C–N), 151.26 (C, Ar–O), 143.45 (C, Ar–N), 130.98 (C, Ar–S), 121.94(C, q, $J = 230$ Hz, $–CF_3$), 119.62 (C, Ar-4), 118.85 (C, Ar-5), 113.98 (C, Ar-7), 54.64 (C, N–C–C), 33.20 (C, $–CH_2–$), 25.42 (C, $–CH_2–$), 24.68 (C, $–CH_2–$); Anal. Calcd for $C_{14}H_{15}F_3N_2OS$: C, 53.15; H, 4.78; N, 8.86. Found: C, 53.33; H, 4.68; N, 8.67.

2-(N-pyrrolidine)-6-trifluoromethoxy-benzothiazole (4f)

White solid; mp 129–130 °C; IR (KBr) υ_{max} 3418, 2969, 2870, 2361, 1614, 1554, 1452, 1365, 1243, 1214, 1184 cm^{-1};

^{1}H NMR ($CDCl_3$, 500 MHz): $\delta = 7.53$ (1H, d, $J =$ 8.8 Hz, Ar–H), 7.46 (1H, s, Ar–H), 7.15 (1H, d, $J = 8.8$ Hz, Ar–H), 3.58 (4H, t, $J = 6.3$ Hz, CH_2–N–CH_2), 2.11–2.06 (4H, m, –CH_2CH_2–); ^{13}C NMR ($CDCl_3$, 100 MHz): $\delta =$ 165.79 (C, S–C–N), 152.15 (C, Ar–O), 142.91 C, Ar–N), 131.35 (C, Ar–S), 121.94(C, q, $J = 235$ Hz, –CF_3), 119.49 (C, Ar-4), 118.74 (C, Ar-5), 113.89 (C, Ar-7), 49.52 (C, N–C–C), 25.61 (C, –CH_2–); Anal. Calcd for $C_{12}H_{11}F_3N_2OS$: C, 49.99; H, 3.85; N, 9.72. Found: C, 49.87; H, 3.75; N, 9.61.

2-(N-piperidine)-6-trifluoromethoxy-benzothiazole (4g)

White solid; mp 74–75 °C; IR (KBr) υ_{max} 3423, 2940, 2859, 2361, 1608, 1549, 1461, 1246, 1158 cm^{-1}; ^{1}H NMR ($CDCl_3$, 500 MHz): $\delta = 7.49$ (1H, d, $J = 8.8$ Hz, Ar–H), 7.45 (1H, s, Ar–H), 7.14 (1H, d, $J = 8.8$ Hz, Ar–H), 3.61–3.60 (4H, m, –CH_2–N–CH_2–), 1.72–1.71 (6H, m, –$CH_2CH_2CH_2$–); ^{13}C NMR ($CDCl_3$, 125 MHz): $\delta = 169.27$ (C, S–C–N), 151.78 (C, Ar–O), 143.17 (C, Ar–N), 131.32 (C, Ar–S), 121.69(C, q, $J = 266.5$ Hz, –CF_3), 119.56 (C, Ar-4), 118.92 (C, Ar-5), 113.80 (C, Ar-7), 49.68 (C, N–C–C), 25.27 (C, –CH_2–), 24.17 (C, –CH_2–); Anal. Calcd for $C_{13}H_{13}F_3N_2OS$: C, 51.65; H, 4.33; N, 9.27. Found: C, 51.46; H, 4.42; N, 9.16.

2-(N-morpholine)-6-trifluoromethoxy-benzothiazole (4h)

White solid; mp 103–105 °C; IR (KBr) υ_{max} 3447, 2974, 2907, 2866, 1608, 1549, 1459, 1380, 1339, 1267, 1112, 1026 cm^{-1}; ^{1}H NMR ($CDCl_3$, 500 MHz): $\delta = 7.52$ (1H, d, $J = 8.8$ Hz, Ar–H), 7.49 (1H, s, Ar–H), 7.17 (1H, d, $J =$ 8.8 Hz, Ar–H), 3.84–3.82 (4H, m, –CH_2–O–CH_2–), 3.63–3.61 (4H, m, –CH_2–N–CH_2–); ^{13}C NMR ($CDCl_3$, 125 MHz): $\delta = 169.45$ (C, S–C–N), 151.22 (C, Ar–O), 143.64 (C, Ar–N), 131.19 (C, Ar–S), 121.65(C, q, $J =$ 223.8 Hz, –CF_3), 119.86 (C, Ar-4), 119.57 (C, Ar-5), 113.98 (C, Ar-7), 66.18 (C, N–C–C), 48.51 (C, –CH_2–); Anal. Calcd for $C_{12}H_{11}F_3N_2O_2S$: C, 47.37; H, 3.64; N, 9.21. Found: C, 47.49; H, 3.54; N, 9.30.

2-(N-4-methyl-1-piperidinyl)-6-trifluoromethoxy-benzothiazole (4i)

White solid; mp 77–78 °C; IR (KBr) υ_{max} 3419, 2940, 2805, 2727, 1614, 1470, 1358, 1271, 1184, 772 cm^{-1}; ^{1}H NMR ($CDCl_3$, 400 MHz): $\delta = 7.47$ (1H, d, $J = 8.7$ Hz, Ar–H), 7.44 (1H, s, Ar–H), 7.13 (1H, d, $J = 8.2$ Hz, Ar–H), 4.09 (2H, d, $J = 12.7$ Hz, N–CH_2–), 3.12 (2H, t, $J = 12.7$ Hz, –CH_2–N), 1.77 (2H, d, $J = 12.7$ Hz, –CH_2–), 1.68–1.63 (1H, m, –CH–), 1.36–1.26 (2H, m, –CH_2–), 1.00 (3H, d, $J = 6.5$ Hz, –CH_3); ^{13}C NMR ($CDCl_3$, 100 MHz): $\delta =$ 169.20 (C, S–C–N), 151.80 (C, Ar–O), 143.18 (C, Ar–N), 131.36 (C, Ar–S), 121.93 (C, q, $J = 231$ Hz, –CF_3), 119.60 (C, Ar-4), 118.94 (C, Ar-5), 113.83 (C, Ar-7), 49.07 (C, N–C–C), 33.43 (C, –CH_2–), 30.79 (C, –CH–), 21.71 (C, –CH_3); Anal. Calcd for $C_{14}H_{15}F_3N_2OS$: C, 53.15; H, 4.78; N, 8.86. Found: C, 53.76; H, 4.60; N, 8.70.

Animals

Six-week-old male Kunming mice (18–22 g, specific pathogen-free grade, SPF) were obtained from the Academy of Experimental Animal Center of The Fourth Military Medical University (Xi'an, China). Mice were maintained under normal conditions: 21–26 °C temperature, 60–70% relative humidity, 12:12 h dark/light cycle, and free access to laboratory standard diet and water. All mice were quarantined and adapted for 7 days after arriving. All animal experiments were conducted under institutional guidelines and approved by the Ethical Committee for Animal Care and Use of the Northwestern Polytechnical University.

Assessment of antinociceptive activity

Antinociceptive activity of the test compounds against noxious thermal stimulation was measured by hot-plate test in mice as described in references (Kaplancikli et al. 2012; Turan-Zitouni et al. 2015; Queiroz et al. 2015). Mice were placed into the hot plate apparatus in a quiet environment and a hot stimulus (55 ± 0.5 °C) used to determine their initial pain threshold. The time (in seconds) that elapsed between placing the mouse on the hot plate and the manifestation of signs of acute discomfort, such as licking of the hind paw or jumping in an attempt to escape from the heat, was taken as the reaction time or latency. The mice pain threshold greater than 60 s or less than 5 s were eliminated.

Statistical analysis

Data were analyzed using SPSS 13.0 version. The results were expressed as the mean ± S.E.M. The data were subjected to one-way analysis of variance (ANOVA) followed by Tukey–Kramer post-hoc analysis. The level of $p < 0.05$ was used as the criterion of statistical significance. $P < 0.01$ was considered extreme significant.

Results and discussion

Synthesis and structural confirmation

These N-alkylated derivatives of riluzole were synthesized according to the synthetic procedure shown in Scheme 1. Although the synthesis route of compound **3** had been

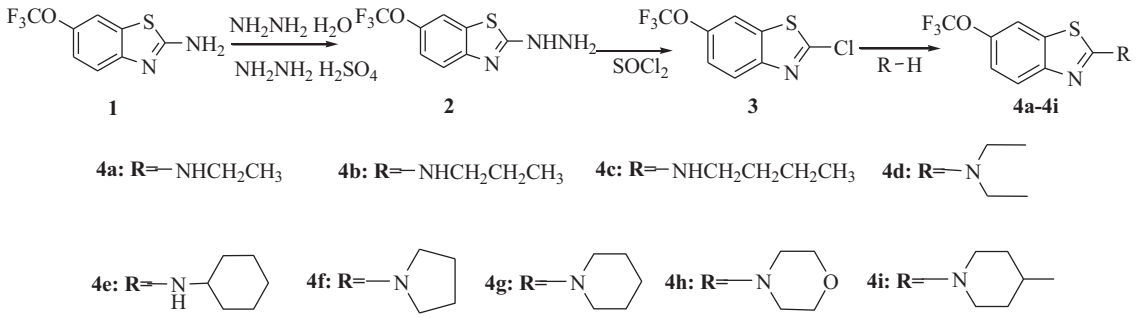

Scheme 1 Synthesis of new N-alkylated derivatives of riluzole

reported, we optimized the synthetic condition and processing method. For example, in the process of preparing compound **2**, the precipitate was vacuum filtered and triturated in a mixture of water-diethyl ether according to the references (Saha et al. 2009; Mignani et al. 1992). We found that the yield was very low by this method because precipitate was not complete. Therefore, our method was that the reaction mixture was poured into ice water. In the process of preparing compound **3**, the residue $SOCl_2$ was destroyed by water. However, it was not a good method. The $SOCl_2$ should be evaporated, then the residue was dissolved in CH_2Cl_2. The CH_2Cl_2 which contains residual $SOCl_2$ was evaporated again. It can be used repeatedly.

In the second step reaction, tail gas absorption equipment was needed. As we can see from Scheme 1, compound 2-chloro-6-trifluoromethoxy benzothiazole (**3**) was an important intermediate. The chlorine atom in compound **3** had high reactivity, so it was very easy to be substituted by the alkylamine. The reagent, reaction time, temperature, yield and melting point were summarized in Table 1 for these N-alkylated derivatives of riluzole.

As can be seen from Table 1, all of the compounds were prepared with high yield (above 75%). The best yield of these compounds could reach to 85.6%. The reaction temperature was 45 °C or room temperature. The reaction conditions were very mild and efficient. In the third step reaction, the alkylamine was not only a substrate but also a solvent. After the completion of the reaction, the alkylamine could be recycled under reduced pressure. Therefore, the solvent was saved owing to its re-use and the environmental pollution was reduced.

Table 1 Preparation of novel N-alkylated derivatives of riluzole

R–H		Temp.	Time	**4**(Yield/%)	m.p.(°C)
1	Ethylamine	45 °C	12 h	**4a** (75.4)	133–134
2	Propylamine	45 °C	4 h	**4b** (79.7)	88–89
3	*n*-Butylamine	45 °C	4 h	**4c** (84.8)	76–78
4	Diaethylamin	45 °C	12 h	**4d** (75.9)	38–39
5	Cyclohexylamine	45 °C	12 h	**4e** (80.3)	96–97
6	Pyrrolidine	rt	3 h	**4f** (85.6)	129–130
7	Piperidine	rt	3 h	**4g** (81.4)	74–75
8	Morpholine	rt	3 h	**4h** (83.3)	103–105
9	4-Methylpiperidine	rt	3 h	**4i** (85.1)	77–78

Crystal structures

Single crystals of compounds **3**, **4e**, **4f**, and **4i** were obtained by recrystallization and their structures were further confirmed by X-ray diffraction determination. The perspectives were shown in Fig. 1. The crystal data, details concerning data collection and structure refinement were listed in Table 2, Bond lengths and angles were listed in Table s1–s4 (See Supplementary data). Crystals of 2-chloro-6-trifluoromethoxy benzothiazole (**3**) were obtained by recrystallization from petroleum ether (bp. 60–90 °C). The crystals of compound **3** were monoclinic, space group P2 (1)/n with four molecules per unit cell. In the crystal structure of compound **3**, the N(1)–C(1) in 0.1268(3) nm was a double bond. However, the N(1)–C(2) in 0.1377(3) nm was a single bond. The bond length of C(1)–Cl(1) was 0.1691(3) nm. The bond length of S(1)–C(1) (0.1722 nm) was longer than S(1)–C(1) (0.1714 nm). It indicated that the S(1) atom lies within the thiazole ring plane was close to benzene ring. The bond lengths of C–F in the $–CF_3$ were different and the values of them were 0.1287, 0.1296, and 0.1303 nm, respectively. The thiazole ring and benzene ring were coplanar.

Crystals of compound 2-(N-pyrrolidine)-6-trifluoromethoxy-benzothiazole (**4f**) were obtained by recrystallization from ethanol. The compound **4f** crystallizes in the triclinic P-1 space group with two molecules per unit cell. The N(1)–C(8) in 0.1299(4) nm was a double bond. The N(1)–C(5) in 0.1378(4) nm was a single bond. The bond length of N(2)–C(8) (0.1328 nm) was shorter than N(2)–C(9) and N(2)–C(12) (0.1457 nm, 0.1453 nm,

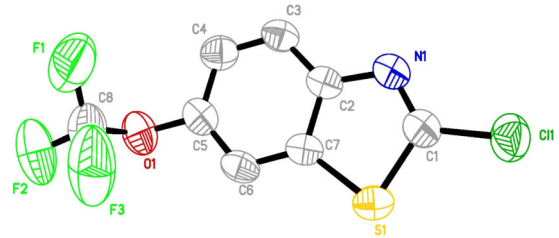

Compound **3**

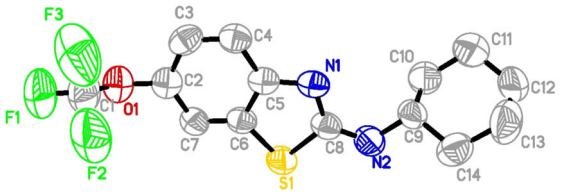

Compound **4e**

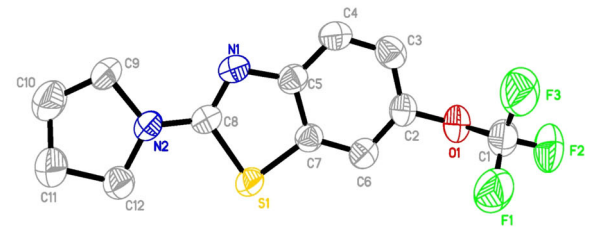

Compound **4f**

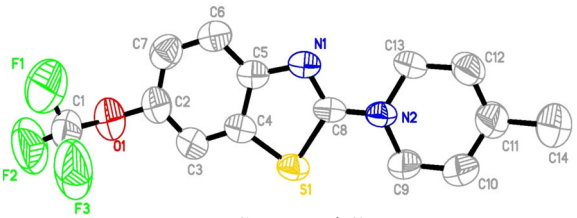

Compound **4i**

Fig. 1 ORTEP drawings of compounds **3**, **4e**, **4f**, and **4i**

respectively), which were belonged to the pyrrolidine ring. The length of C(3)–C(2) and C(5)–C(4) in benzene ring were 0.1732 and 0.1383 nm, respectively.

Crystals of compounds **4e** and **4i** were obtained by recrystallization from ethanol. The compound **4e** crystallize in the monoclinic P21/n space group with four molecules per unit cell and the compound **4i** in the triclinic P-1 space groups. They had same properties in bond length. In addition, the cyclohexane ring of compound **4e** and the piperidine ring of compound **4i** were typical chair conformation. The piperidine ring was in the same plane with benzothiazole ring. However, there was a dihedral angle between the mean plane of benzothiazole and cyclohexane ring.

The packing drawing of compounds **3**, **4e**, **4f**, and **4i** were given in the supplementary data (Figs. s1–s4). In the crystal packing, as shown in Fig. s3 in supplementary data, weak intermolecular hydrogen bonds are observed (showed as dashed lines). In the crystal packing, as shown in Figs. s3 and s4, adjacent molecules were crossed stacked through strong offset π···π aromatic stacking interactions. The crystal structures have potential applications in identifying the binding site for allosteric modulators of the receptor, and should be useful in the area of medical or pharmaceutical applications.

Hot plate test

This study investigated the antinociceptive activity of some N-alkylated derivatives of riluzole by hot plate test in mice. Figure 2 showed the antinociceptive effects of **4b**, **4c**, **4g**, and **4h** at different doses on the time mice spent on the hot plate. Compound **4b**, at the doses tested (6 mg/kg: 17.06 ± 4.72 s; 12 mg/kg: 17.60 ± 4.01 s), showed extreme significant increase in the time mice spent on the hot plate when compared with the control group (7.96 ± 2.13 s) (Fig. 2 compound **4b**). At the doses tested (18 mg/kg: 13.78 ± 2.89 s; 36 mg/kg: 13.61 ± 2.43 s), compound **4b** showed significant increase in the reaction time. Compound **4c**, at all the doses tested, showed extreme significant increase in the reaction time when compared with the control group (Fig. 2 compound **4c**).

Compound **4h**, at the doses tested (6 mg/kg: 12.90 ± 2.58 s; 12 mg/kg: 14.89 ± 2.32 s), showed extreme significant increase in the reaction time compared with the control group 9.06 ± 2.02 s). Compound **4h**, at the dose 18 mg/kg i.g had a significant increase in the reaction time (12.89 ± 2.94 s) compared with the control group at dose 0 mg/kg (9.06 ± 2.02 s). Compound **4g**, only at the dose 12 mg/kg i.g had a significant increase in the reaction time (13.37 ± 4.24 s) compared with the control group at dose 0 mg/kg (9.07 ± 2.65 s).

Animals treated with riluzole (compound **1**) showed increased latency time on the hot plate. From the Fig. 3, riluzole had a significant effect on antinociceptive activity. At a dose of 18 mg/kg, it had showed extreme significant increase in latency time (15.40 ± 2.83 s). When the intragastric administration dose arrived at 24 mg/kg, the average of latency time (14.13 ± 2.99 s) did not increase with the addition of the doses.

According to our previous study, we chose the same dose (18 mg/kg) to compare antinociceptive activity (See Fig. 4). The blank solvent group (**BL**) and compound **1** (riluzole) were control group and positive control group, respectively. Compared to the control group (0 mg/kg, BL), the effect of compounds **4b** and **4h** showed a significant increase (13.78 ± 2.89 s, 12.89 ± 2.94 s, respectively).

Table 2 Crystal data and structure refinement for **3**, **4e**, **4f**, and **4i**

	Compound **3**	Compound **4e**	Compound **4f**	Compound **4i**
CCDC deposit no.	1039246	1453892	1045917	1446747
Empirical formula	$C_8H_3ClF_3NOS$	$C_{14}H_{15}F_3N_2OS$	$C_{12}H_{11}F_3N_2OS$	$C_{14}H_{15}F_3N_2OS$
Formula weight	252.96	316.34	288.29	316.34
Temperature (K)	296(2)	296(2)	296(2)	296(2)
Wavelength (nm)	0.071073	0.071073	0.071073	0.071073
Crystal system	Monoclinic	Monoclinic	Triclinic	Triclinic
Space group	P2(1)/n	P2(1)/n	P-1	P-1
a (nm)	1.1797(10)	1.3401(5)	0.71573(16)	0.6893(2)
b (nm)	1.1152(10)	1.0138(4)	0.80484(14)	0.8216(2)
c (nm)	0.7379(7)	1.3401(5)	1.1949(3)	1.4252(4)
α (°)	90	90	91.291(4)	88.664(5)
β (°)	99.856	97.19	99.683(4)	79.693(4)
γ (°)	90	90	111.850(3)	72.664(5)
Volume (nm^3)	0.9565	0.18062(4)	0.627	0.7577(4)
Z	4	4	2	2
D_{calc} (g/cm^3)	1.761	1.325	1.516	1.382
Abs.coefficient (mm^{-1})	0.632	0.218	0.285	0.245
F(000)	504	752	294	326
Crystal size (mm^3)	0.37 × 0.28 × 0.20	0.37 × 0.31 × 0.24	0.37 × 0.29 × 0.130	0.35 × 0.30 × 0.24
θ limit (°)	1.75 to 25.10	2.03 to 25.10	1.74 to 25.10	1.45 to 25.10
Ranges/indices h. k. l.	−9/14, −13/13, −8/7	−15/15, −12/11, −15/13	−5/8, −9/9, −14/13	−8/7, −9/9, −16/11
Reflections collected/ unique/R_{int}	4644 / 1706 /0.0268	6197 / 2559/ 0.0472	3107 / 2206/ 0.0170	3809 / 2680/ 0.0206
Completeness to θ = 25.10°	100.0 %	80.1 %	98.7 %	99.1 %
Data/restraints/ parameters	1706 / 0 / 136	2680 / 0 / 191	2206 / 0 / 172	2680 / 0 / 191
Goodness of fit on F^2	1.081	1.018	1.108	1.026
R_1, wR_2	0.0446, 0.0953	0.0694, 0.1847	0.0617, 0.1591	0.0735, 0.2161
Largest diff. peak and hole ($e•nm^{-3}$)	311 and −271	314 and −179	307 and −306	517 and −336

Compounds **4c**, **4f**, and **4i** showed extreme significant increase (18.07 ± 3.08 s, 17.75 ± 3.23 s, and 15.36 ± 2.01 s, respectively) in the reaction time when compared to the control group. However, at the dose of 18 mg/kg, no significant differences were observed for the riluzole and compounds **4c**, **4f**, **4i**.

To compare the antinociceptive activity with riluzole, the difference values were calculated by subtracting the riluzole latency from the latency of **4a**–**4i** (See Fig. 5). The positive value indicated the analgesic effect was better than riluzole, but the negative value indicated it was worse than riluzole. As we can see, compounds **4c** and **4f** showed extreme significant analgesic effect compared to the riluzole. The 2-substituent groups of them were *n*-butylamine and pyrrolidine, respectively. They all have four carbon atoms in substituent group. The analgesic effect of compound **4i** was the same as riluzole. However, the antinociceptive activities of other compounds were worse than riluzole.

Several lines of evidence had shown that nociception in the hot plate test results from the accumulation of intracellular Ca^{2+} concentration that, in turn, initiates a number of second / third messenger- mediated intracellular cascades (Sommer and Seeburg 1992). Riluzole can stabilize Na^+ channels and inhibit glutamate release. Riluzole can also inhibit Ca^{2+}-dependent release of glutamate from neurons, as well as interact with other cellular targets (Gegelashvili and Bjerrum 2014). Therefore, our hot plate test results suggested that the possible mechanisms of these title

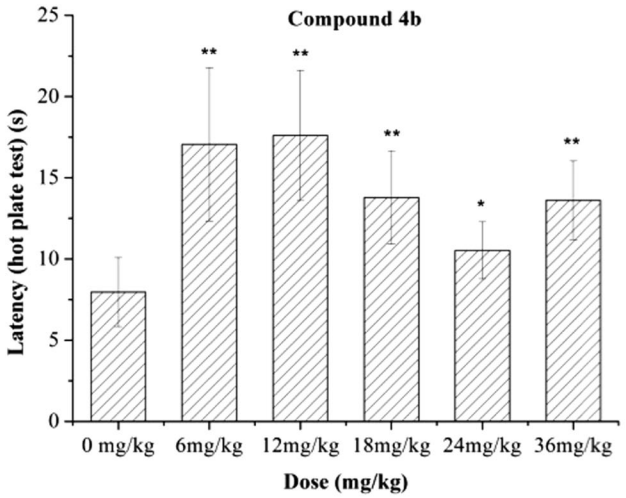

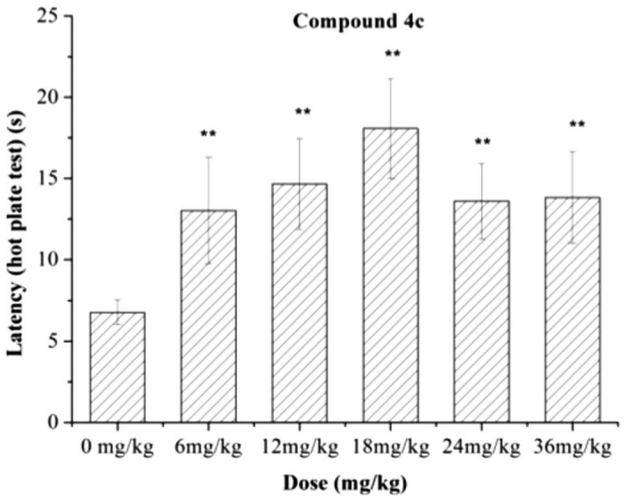

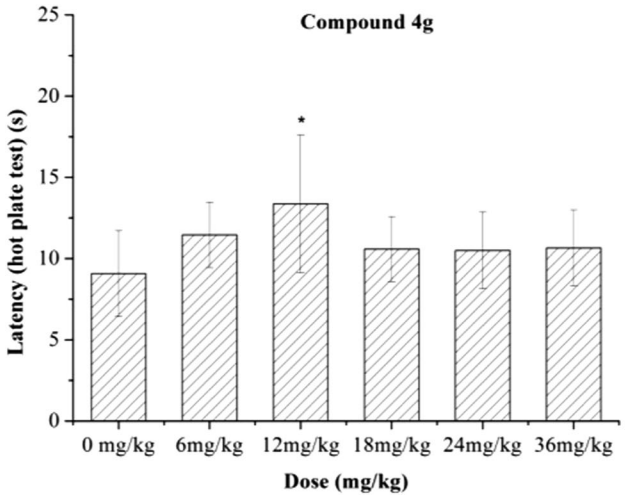

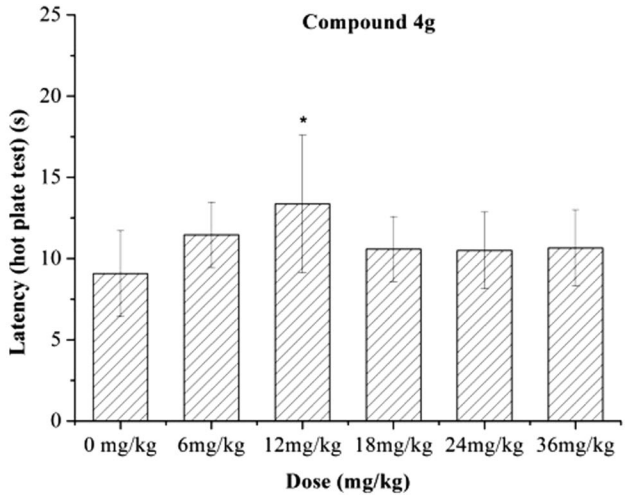

Fig. 2 The relationship between latency and intragastric administration concentration of compound **4b**, **4c**, **4g**, and **4h**. ** $p < 0.01$ compared with the 0 mg/kg group, * $p < 0.05$ compared with the 0 mg/kg group. Each bar is the mean ± S.E.M. of individual determinations in 8 mice of each group

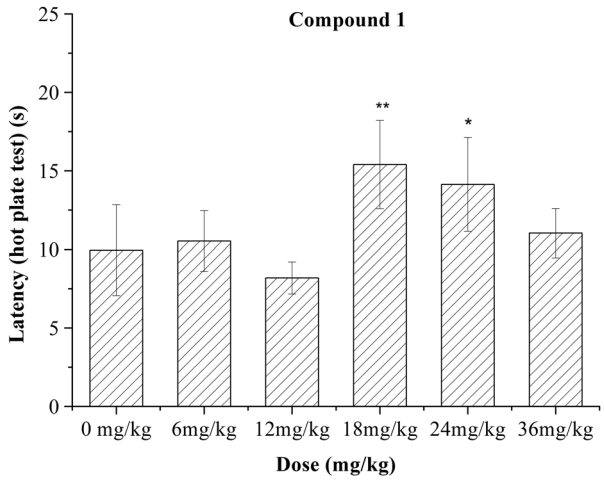

Fig. 3 The relationship between latency and intragastric administration concentration of compound **1** (riluzole). ** $p < 0.01$ compared with the 0 mg/kg group, * $p < 0.05$ compared with the 0 mg/kg group. Each bar is the mean ± S.E.M. of individual determinations in 8 mice of each group

compounds may be linked to Na^+ channels, Ca^{2+} concentration or glutamate release.

Conclusion

In conclusion, we have reported a practical synthetic route towards N-alkylated derivatives of riluzole. New single crystals of compounds **3**, **4e**, **4f**, and **4i** were obtained by recrystallization and their structures data were very useful in the area of medical or pharmaceutical applications. To our knowledge, with exception of compounds **2**, **3**, **4a**, and **4c**, others have not been reported by references. The results showed that **4c**, **4f**, and **4i** had increased the latency time compared to the blank solvent group. They have potential application in developing new drug candidates with anti-nociceptive activity.

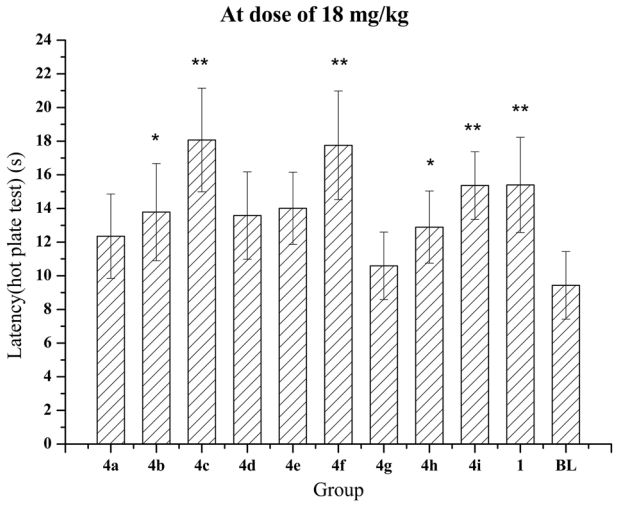

Fig. 4 Antinociceptive activity of compounds **4a–4i** and **1**, at the dose of 18 mg/kg in the hot-plate test. $^{**}p < 0.01$ compared with the **BL** group, $^{*}p < 0.05$ compared with the **BL** group. Each bar is the mean ± S.E.M. of individual determinations in 8 mice of each group

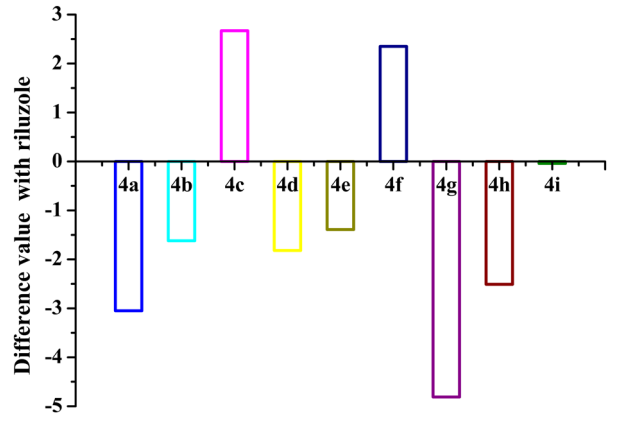

Fig. 5 Antinociceptive activities of **4a–4i** compared with riluzole, at the dose of 18 mg/kg in the hot-plate test. The difference values were calculated by subtracting the riluzole latency from the latency of **4a–4i**. The positive value indicated the analgesic effect was better than riluzole, but the negative value indicated it was worse than riluzole

Acknowledgements The work was supported by the National Natural Science Foundation of China (No. 21202130), the Fundamental Research Funds for the Central Universities (No. 3102014JCQ15005), the Natural Science Foundation Research Project of Shaanxi Province (No. 2015JM2067), the Seed Foundation of Innovation and Creation for Graduate Students in Northwestern Polytechnical University (No. Z2017239), the national innovation experiment program for university students (No.201610699258)

Compliance with ethical standards

Conflict of interest The authors declare that they have no conflict of interest.

References

Cheah BC, Vucic S, Krishnan AV, Kiernan MC (2010) Riluzole, neuroprotection and amyotrophic lateral sclerosis. Curr Med Chem 17:1942–1959

Cheung YK, Gordon PH, Levin B (2006) Selective promising ALS therapies in clinical trials. Neurology 67:1748–1751

Chew DJ, Carlstedt T, Shortland PJ (2014) The effects of minocycline or riluzole treatment on spinal root avulsion-induced pain in adult rats. J Pain 5:664–675

Coleman N, Nguyen HM, Cao Z, Brown BM, Jenkins DP, Zolkowska D, Chen YJ, Tanaka BS, Goldin AL, Rogawski MA, Pessah IN (2015) The riluzole derivative 2-amino-6-trifluoromethylthiobenzothiazole (SKA-19), a mixed $K_{Ca}2$ activator and Na_V blocker, is a potent novel anticonvulsant. Neurotherapeutics 12:234–249

Domino EF, Unna KR, Kerwin J (1952) Pharmacological properties of benzazoles. I. Relationship between structure and paralyzing action. J Pharmacol Exp Ther 105:486–497

Gegelashvili G, Bjerrum OJ (2014) High-affinity glutamate transporters in chronic pain: an emerging therapeutic target. J Neurochem 131:712–730

Jehle T, Bauer J, Blauth E, Hummel A, Darstein M, Freiman TM, Feuerstein TJ (2000) Effects of riluzole on electrically evoked neurotransmitter release. Br J Pharmacol 130:1227–1234

Jimonet P, Audiau F, Barreau M, Blanchard JC, Boireau A, Bour Y, Mignani S (1999) Riluzole series. Synthesis and in vivo "anti-glutamate" activity of 6-substituted-2-benzothiazolamines and 3-substituted-2-imino- benzothiazolines. J Med Chem 42:2828–2843

Joyce LL, Batey RA (2009) Heterocycle formation via palladium-catalyzed intramolecular oxidative C−H bond functionalization: an efficient strategy for the synthesis of 2-aminobenzothiazoles. Org Lett 11:2792–2795

Kaplancikli ZA, Altintop MD, Turan-Zitouni G, Ozdemir A, Can OD (2012) Synthesis and analgesic activity of some acetamide derivatives. J Enzym Inhib Med Chem 27:275–280

Liu AY, Mathur R, Mei N, Langhammer CG, Babiarz B, Firestein BL (2011) Neuroprotective drug riluzole amplifies the heat shock factor 1 (HSF1)- and glutamate transporter 1 (GLT1)-dependent cytoprotective mechanisms for neuronal survival. J Biol Chem 286:2785–2794

Mignani S, Audiau F, Blevec JL (1992) Versatile methods for the synthesis of 2-amino-6-trifluoromethoxy-(nitro) benzothiazoles. Synth Commun 22:2769–2780

Mishra SP, Shukla SK, Pandey BL (2014) A preliminary evaluation of comparative effectiveness of riluzole in therapeutic regimen for irritable bowel syndrome. Asian Pac J Trop Biomed 4:S335–340

Mizoule J, Meldrum B, Mazadier M, Croucher M, Ollat C, Uzan A (1985) 2-Amino-6-trifluoromethoxy benzothiazole, a possible antagonist of excitatory amino acid neurotransmission—I: Anticonvulsant properties. Neuropharmacol 24:767–773

Moon ES, Karadimas SK, Yu WR, Austin JW, Fehlings MG (2014) Riluzole attenuates neuropathic pain and enhances functional recovery in a rodent model of cervical spondylotic myelopathy. Neurobiol Dis 62:394–406

Nicholson KJ, Zhang S, Gilliland TM, Winkelstein BA (2014) Riluzole effects on behavioral sensitivity and the development of axonal damage and spinal modifications that occur after painful nerve root compression. J Neurosurg Spine 20:751–762

Queiroz RB, Carvalho FL, Fonsêca DV, Barbosa-Filho JM, Salgado PR, Paulo LL, Queiroz AB, Pordeus LC (2015) Antinociceptive effect of hydantoin 3-phenyl-5-(4 -ethylphenyl)- imidazolidine-2, 4-dione in mice. Molecules 20:974–986

Rana A, Siddiqui N, Kahn SA (2007) Benzothiazoles: a new profile of biological activities. Indian J Pharm Sci 69:10–17

Saha P, Ramana T, Purkait N, Ali MA, Paul R (2009) Ligand-free copper-catalyzed synthesis of substituted benzimidazoles, 2-aminobenzimidazoles, 2-aminobenzothiazoles, and benzoxazoles. J Org Chem 74:8719–8725

Sommer B, Seeburg PH (1992) Glutamate receptor channels: novel properties and new clones. Trends Pharmacol Sci 13:291–296

Turan-Zitouni G, Yurttaş L, Kaplancikli ZA, Can OD (2015) Synthesis and anti-nociceptive, anti-inflammatory activities of new aroyl propionic acid derivatives including N-acylhydrazone motif. Med Chem Res 24:2406–2416

Wilson JR, Fehlings MG (2013) Riluzole for acute traumatic spinal cord injury: a promising neuroprotective treatment strategy. World Neurosurg 81:825–829